

ISTITUTO NAZIONALE DI RICERCA METROLOGICA Repository Istituzionale

Single-Photon Emitters in Lead-Implanted Single-Crystal Diamond

Original

Single-Photon Emitters in Lead-Implanted Single-Crystal Diamond / Ditalia Tchernij, S.; Lühmann, T.; Herzig, T.; Küpper, J.; Damin, A.; Santonocito, S.; Signorile, M.; Traina, P.; Moreva, E.; Celegato, F.; Pezzagna, S.; Degiovanni, I. P.; Olivero, P.; Jakšić, M.; Meijer, J.; Genovese, M.; Forneris, J.. - In: ACS PHOTONICS. - ISSN 2330-4022. - 5:12(2018), pp. 4864-4871. [10.1021/acsphotonics.8b01013]

Availability:

This version is available at: 11696/60001 since: 2021-02-01T14:06:37Z

Publisher:

ACS-American Chemical Society

Published

DOI:10.1021/acsphotonics.8b01013

Terms of use:

This article is made available under terms and conditions as specified in the corresponding bibliographic description in the repository

Publisher copyright

(Article begins on next page)

Single-Photon Emitters in Lead-Implanted Single-Crystal Diamond

S. Ditalia Tchernij,^{†,‡,¶} T. Lühmann,^{§,¶} T. Herzig,[§] J. Küpper,[§] A. Damin,^{||} S. Santonocito,[†] M. Signorile,^{||} P. Traina,[⊥] E. Moreva,[⊥] F. Celegato,[⊥] S. Pezzagna,[§] I. P. Degiovanni,[⊥] P. Olivero,^{†,‡} M. Jakšić,[#] J. Meijer,[§] P. M. Genovese,^{‡,⊥} and J. Forneris^{*,‡,¶,||}

[†]Physics Department and “NIS” Inter-departmental Centre, University of Torino, Torino 10124, Italy

[‡]Istituto Nazionale di Fisica Nucleare (INFN), Sez. Torino, Torino 10125, Italy

[§]Department of Nuclear Solid State Physics, Leipzig University, Leipzig 04109, Germany

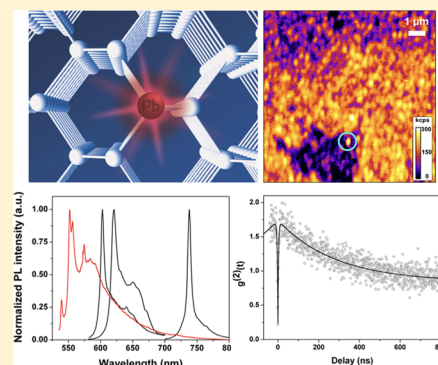
^{||}Chemistry Department and “NIS” Inter-departmental Centre, University of Torino, Torino 10125, Italy

[⊥]Istituto Nazionale di Ricerca Metrologica (INRiM), Torino 10135, Italy

[#]Ruder Bošković Institute, Zagreb 10000, Croatia

ABSTRACT: We report on the creation and characterization of Pb-related color centers in diamond upon ion implantation and subsequent thermal annealing. Their optical emission in the photoluminescence (PL) regime consists of an articulated spectrum with intense emission peaks at 552.1 and 556.8 nm, accompanied by a set of additional lines in the 535–700 nm range. The attribution of the PL emission to stable Pb-based defects is corroborated by the correlation of its intensity with the implantation fluence of Pb ions. PL measurements performed as a function of sample temperature (in the 143–300 K range) and under different excitation wavelengths (i.e., 532, 514, 405 nm) suggest that the complex spectral features observed in Pb-implanted diamond might be related to a variety of different defects and/or charge states. The emission of the 552.1 and 556.8 nm lines is reported at the single-photon emitter level, demonstrating that they originate from the same individual defect. This work follows from previous reports on optically active centers in diamond based on group-IV impurities, such as Si, Ge, and Sn. In perspective, a comprehensive study of this set of defect complexes could bring significant insight on the common features involved in their formation and opto-physical properties, thus offering a basis for the development of a new generation of quantum-optical devices.

KEYWORDS: diamond, lead, color centers, single-photon source, ion implantation, photoluminescence



Diamond is a promising platform for the development of solid-state quantum devices with applications in quantum information processing and sensing.^{1–5} In recent years, the search for optically active defects with appealing properties has led to the discovery of several classes of color centers^{6–11} alternative to the widely investigated negatively charged nitrogen-vacancy complex (NV[−] center).¹² This is motivated by the fact that the NV[−] defect, although extremely promising for its peculiar spin features,¹³ is limited in several applications by suboptimal opto-physical properties, such as a spectrally broad emission with intense phonon sidebands, the presence of charge state blinking, and a relatively low emission rate.^{14–16} In particular, the silicon-vacancy center (SiV)¹⁷ has attracted significant attention due to a near transform-limited emission,^{18,19} good photon indistinguishability,^{19,20} the capability of coherently controlling its spin properties,^{21–24} and the emergence of reliable techniques for its deterministic fabrication.^{25–28}

The recently explored emitters related to group-IV impurities, such as the germanium-related (GeV)^{29–31} and tin-related (SnV)^{32–34} color centers, are characterized by

similar defect structure and opto-physical properties to those of the SiV center, such as photostability, narrow zero-phonon line (ZPL), relatively small phonon coupling, and high emission rate. This brings further interest in this class of optically active defects. In particular, these recent discoveries open the question of whether the whole set of group-IV-based complexes (SiV, GeV, SnV, and now PbV) result in stable optically active emitters, and second whether the properties of these color centers exhibit any common features.

In this work, we present evidence of photoluminescence (PL) emission from color centers created upon the implantation of Pb ions in diamond followed by thermal annealing. To the best of the authors' knowledge, in a recent work³⁵ promisingly similar results were obtained from low-fluence Pb implantations in diamond, although with several differences, which could be ascribed to different experimental conditions (excitation wavelengths, spectral filtering, measurement temperature).

Received: July 24, 2018

Published: November 12, 2018

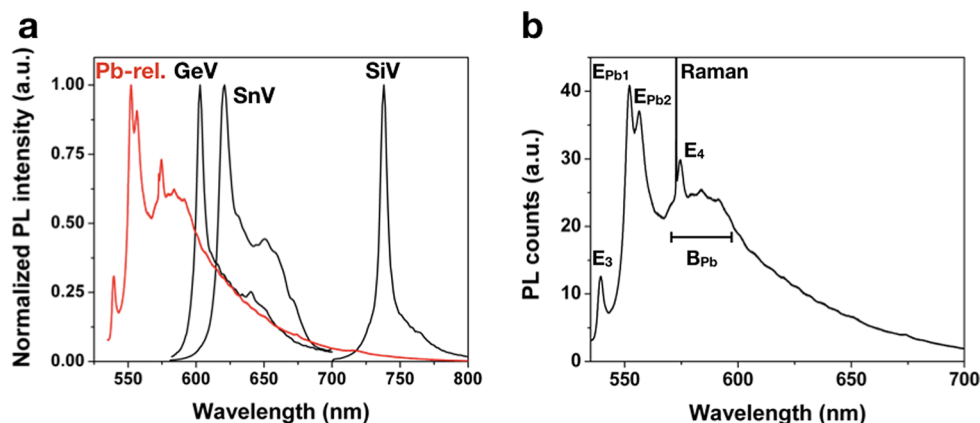


Figure 1. (a) PL emission spectra under 532 nm laser excitation from group-IV-related impurities upon ion implantation in the $(1\text{--}10) \times 10^{12} \text{ cm}^{-2}$ fluence range: SiV (ZPL at 738 nm), GeV (602 nm), SnV (620 nm), and the newly reported Pb-related (main emission line at $\sim 552 \text{ nm}$, red curve) centers. (b) Typical PL spectrum under 532 nm laser excitation of a detector-grade diamond substrate (sample #1) implanted with 30 keV PbO_2^- ions at a $2 \times 10^{13} \text{ cm}^{-2}$ fluence.

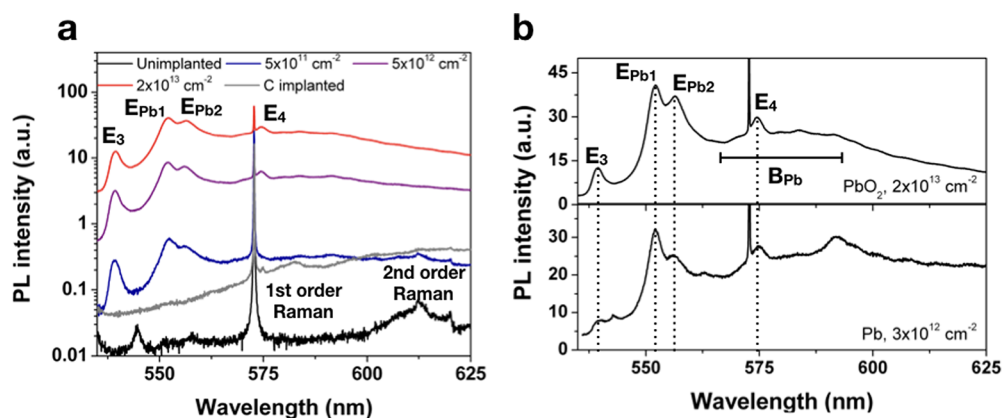


Figure 2. (a) PL emission spectra under 532 nm laser excitation of PbO_2^- -implanted diamond (sample #3) at increasing ion fluences in the $(5\text{--}200) \times 10^{11} \text{ cm}^{-2}$ range (red, purple, and blue lines). Additional PL spectra acquired from different regions of the same substrate are reported for the sake of comparison: unirradiated diamond (black line) and implanted with 15 keV C^- ($3 \times 10^{15} \text{ cm}^{-2}$ fluence, gray line). (b) PL spectra under 532 nm laser excitation of diamond implanted with 30 keV PbO_2^- (sample #1) and 15 keV Pb^- ions (sample #3), respectively, at 2×10^{13} and $3 \times 10^{12} \text{ cm}^{-2}$ fluences.

ENSEMBLE PL EMISSION

Samples Processing. The defect fabrication was performed by implanting 35 keV PbO_2^- (sample #1) and 20 keV Pb^- (samples #2, #3) ions at different fluences in three CVD-grown single-crystal IIa diamond substrates supplied by ElementSix. The substrates were characterized respectively by “electronic” (substitutional N and B concentration: $[\text{N}_\text{s}] < 5 \text{ ppb}$, $[\text{B}_\text{s}] < 5 \text{ ppb}$, samples #1 and #2 in the following) and “optical” ($[\text{N}_\text{s}] < 1 \text{ ppm}$, $[\text{B}_\text{s}] < 0.05 \text{ ppm}$, sample #3) grades. The utilization of a PbO_2^- beam was motivated by the low electron affinity of Pb, resulting in relatively small and highly unstable currents achievable for the implantation of elemental ions.³⁶ The chosen molecular beam thus ensured the achievement of relatively higher implantation fluences for the ensemble characterization of Pb-related defects.

Additional implantations of group-IV-related elements were performed to provide a suitable comparison in the present study: 50 keV Si^- ($5 \times 10^{12} \text{ cm}^{-2}$ ion fluence, sample #1), 40 keV Ge^- ($1 \times 10^{13} \text{ cm}^{-2}$, sample #3), and 60 keV Sn^- ($1 \times 10^{12} \text{ cm}^{-2}$, sample #1). The implantation was followed by a thermal annealing at 1200 °C under vacuum (2 h) and by an oxygen plasma treatment, which ensured the removal of

background fluorescence associated with graphitic and organic contaminations of the sample surface.

Room-Temperature PL Emission. A typical room-temperature PL spectrum acquired by confocal microscopy from an ensemble of centers in sample #1 ($2 \times 10^{13} \text{ cm}^{-2}$ implantation fluence) under 532 nm laser excitation is reported in Figure 1 (red line), together with those of SiV (ZPL at 738 nm), GeV (602 nm), and SnV (620 nm) centers (black lines) for the sake of comparison. The most apparent spectral features associated with Pb implantation (Figure 1b) consist of an intense doublet at 552.1 nm (labeled as E_{Pb1} in the following) and 556.8 nm (E_{Pb2}) followed by a broader emission band (B_{Pb}) roughly comprised between 565 and 600 nm. These spectral structures show a striking resemblance to that observed for the SiV, GeV, and SnV centers, where the emission is mainly concentrated at the ZPL, with a less pronounced phonon sideband. Indeed, a common trend in the reported spectra is represented by the fact that the intensity of the phonon sidebands increases for heavier impurities (Figure 1a). Furthermore, the heaviest known group-IV-related center reported before the present work, i.e., the SnV defect, also displays a ZPL doublet fine structure at cryogenic temperatures, indicating that the center could have a split ground

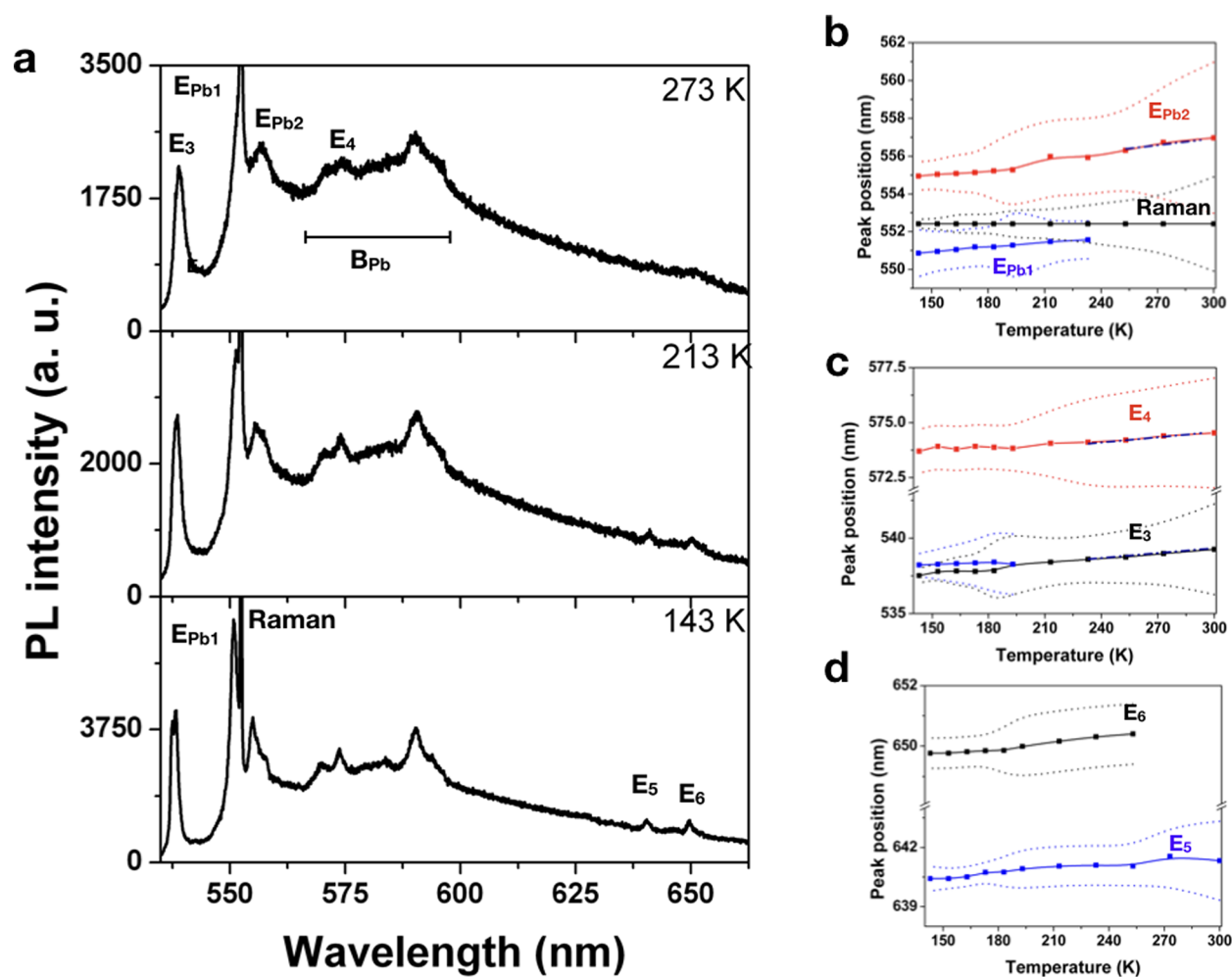


Figure 3. Temperature-dependent PL spectroscopy under 514 nm laser excitation from PbO_2^- -implanted diamond: (a) Pb-related emission in the 535–600 nm spectral range at 273, 213, and 143 K; temperature-dependent ZPL position of (b) E_{Pb1} , E_{Pb2} , and first-order Raman emissions; (c) E_3 and E_4 emission, the former displaying a fine structure at $T < 200$ K; (d) E_5 and E_6 emissions. The dotted lines delimit the fwhm's of the corresponding peaks. The dashed-dotted lines indicate the linear fit of the emission shift.

(and/or excited) state. Apart from this, it is worth remarking that the ZPL wavelength does not follow a systematic spectral shift when considering heavier impurities. This observation is in line with the theoretical calculations reported in ref 37 despite a noticeable mismatch with the experimental value of the ZPL. In addition to the aforementioned spectral features, less intense sharp lines are observed at 539.4 and 574.5 nm (E_3 and E_4 peaks in the following).

A spectral feature similar to the E_3 line has previously been reported in natural diamond upon ion irradiation and high-temperature (>1400 °C) annealing, and tentatively attributed to interstitial-carbon-related defect complexes.¹⁶ However, these previous observations were limited to the cathodoluminescence regime, and the lack of clear evidence of its activity under PL excitation cannot rule out the attribution of the E_3 spectral line to a Pb-related defect.

Conversely, the E_4 emission is tentatively attributed on the basis of temperature-dependent measurements (see below) to the ZPL of the NV^0 center, formed upon the introduction of vacancies in the diamond lattice and the subsequent thermal process. It is also worth mentioning that additional room-temperature spectra acquired in the 700–750 nm range under 532 nm excitation (not shown here) did not reveal any PL

emission around ~ 715 nm, differently from what was reported in ref 35.

Attribution to Pb-Related Lattice Defects. In order to attribute the spectral features reported in Figure 1 to Pb-related color centers, in sample #1 the intensity of the PL emission was correlated with the implantation fluence in the $(5\text{--}200) \times 10^{11} \text{ cm}^{-2}$ range. The corresponding PL spectra are shown in Figure 2a. The aforementioned E_{Pb1} – E_{Pb2} and B_{Pb} features are absent in the spectrum acquired from a pristine reference region of the substrate, and conversely they exhibit a systematically increasing intensity at increasing implantation fluences. Furthermore, the absence of the E_{Pb1} and E_{Pb2} lines is apparent in a control spectrum acquired from a region of the same diamond substrate implanted with 15 keV C^- ions ($3 \times 10^{15} \text{ cm}^{-2}$ fluence, Figure 2a). It is also worth remarking that the E_{Pb1} and E_{Pb2} emission lines have never been observed in previous reports on diamond crystals implanted with light (H, He) or carbon ions, as well as with other heavier ion species,^{5,6,16,38} thus indicating that these spectral features cannot be attributed to intrinsic radiation-induced defects and that the Pb impurities are directly involved in the formation of stable color centers.

Pb^- vs PbO_2^- Ion Implantation. The aforementioned data were acquired on a PbO_2^- -implanted substrate. We show

in Figure 2b that the reported spectral features (E_{Pb1} , E_{Pb2} , E_3 , E_4) are left unchanged for both PbO_2^- and Pb^- ion implantations. This represents an additional experimental evidence that confirms their attribution to Pb-related optical centers and that the presence of implanted O ions does not modify the relevant emission features, at least for the adopted thermal processing parameters. This result also has a significant technical relevance since, in the perspective of the systematic employment of ion implantation for the creation of Pb-related defects, the technical challenges in the transport and acceleration of a stable Pb^- beam could significantly affect the fluence control for the deterministic creation of color centers at low implantation fluences. In this sense, apart from providing a useful contribution to unequivocally attribute the luminescent centers to Pb-based defects, the employment of a PbO_2^- beam also offers a convenient technological solution for the practical fabrication of these defects with ion implantation by taking advantage of more stable ion beams and higher currents.

Temperature-Dependent PL Emission. In order to better investigate the fine structure of the spectral features observed in Pb-implanted diamond, PL spectra under 514 laser excitation were acquired at temperatures in the range comprised between 143 and 273 K (Figure 3a). As typically observed in low-temperature PL experiments, the E_{Pb1} , E_{Pb2} , E_3 , and E_4 PL peaks increase in intensity and reduce their spectral width with respect to room temperature. All the relevant Pb-related emission peaks display a blue-shift at decreasing temperature (Figure 3b–d). This observation is in qualitative agreement with the attribution of the PL peaks to stable lattice defects, whose chemical bonds are shortened at decreasing temperature.³⁹ It is worth noting that at 273 K the main emission peak E_{Pb1} overlaps with the first-order Raman line (552.4 nm) under 514 nm excitation, and its spectral position can be accurately determined only at temperatures below 233 K. As the temperature decreases, its position reaches a value of 550.9 nm at 143 K. Similarly, at the same temperature the E_{Pb2} and the E_4 peak blue-shift to 554.9 and 573.7 nm (Figure 3a,b), respectively. None of these emissions exhibit a fine structure in the probed temperature range. The E_{Pb2} , E_3 , and E_4 peaks exhibit a linear temperature-dependent shift in the 250–300 K range. This behavior is in good agreement with the linear dependence observed in the same temperature range in previous reports for the other group-IV-related color centers in diamond.^{40–42} A linear fitting (dashed green lines in Figure 3b–d) was therefore performed in this temperature interval to provide a preliminary assessment and comparison. The E_{Pb2} and the E_3 peak displayed respective slopes of 12 ± 5 and 12 ± 1 pm K⁻¹, corresponding to 47 ± 5 and 46 ± 5 $\mu\text{eV K}^{-1}$. These values are in the same range (i.e., 9–14 pm K⁻¹) as those reported for the SiV, GeV, and SnV centers.^{40–42} Furthermore, the compatible energy shift of the E_{Pb2} and E_3 lines suggests that the emission might originate from the very same defect complex. Conversely, the E_4 temperature shift of 6 ± 1 pm K⁻¹ (corresponding to 29.7 ± 3 $\mu\text{eV K}^{-1}$) indicates that the emission might be related to a different lattice defect, as supported by the following investigation at the single-photon emitter level. Moreover, this value is comparable with the value of 6.8 ± 0.1 pm K⁻¹ obtained from a linear fitting of the data reported in ref 43 on the temperature dependence of the NV⁰ center. On the basis of this agreement, as well as of the striking similarity in the spectral position at 575 nm, the safest attribution of the E_4

peak is therefore the ZPL of the NV⁰ center, as suggested in ref 35, despite the fact that its peculiar phonon sidebands at higher wavelengths could not be unambiguously observed in our PL spectra. A systematic study of the E_{Pb1} (partially overlapping with the first-order Raman line) was not possible, as the emission of the latter displayed a low intensity in the 250–300 K range, i.e., where a linear behavior is expected.⁴²

Conversely, at 143 K the E_3 peak reveals a splitting into two separate lines (i.e., 537.5 and 538.2 nm, Figure 3c). An additional emission peak located at ~ 592 nm is superimposed to the second-order Raman features (~ 590 –600 nm) and lies in the same spectral position of radiation-induced defects in diamond based on interstitials.⁴⁴ Therefore, an estimation of its intensity trend at decreasing temperatures and its unambiguous interpretation in relation to the E_{Pb1} – E_{Pb2} lines were not possible.

Finally, it is worth remarking that at 143 K two additional spectral lines (i.e., 640.4 and 649.8 nm, labeled as E_5 and E_6 in the following) become visible. Consistently with the above-reported peaks, these spectral features also exhibit a blue-shift at decreasing temperatures (Figure 3d). Furthermore, they were also detected under 405 nm laser excitation, as will be discussed in the following.

PL under 405 nm Laser Excitation. Figure 4 shows a typical room-temperature PL spectrum in the 450–675 nm

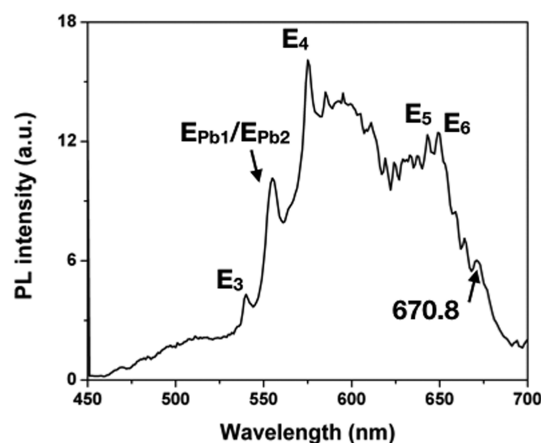


Figure 4. Ensemble PL emission from sample #1 (PbO_2^- implantation fluence: $2 \times 10^{13} \text{ cm}^{-2}$) acquired under 405 nm laser excitation.

range acquired under 405 nm laser excitation with a >450 nm long-pass filter. Most notably, the intense emission doublet at 520 nm reported in ref 35 as the ZPL of the PbV center could not be observed.

The E_{Pb1} , E_{Pb2} , and E_3 peaks are still visible, although with a reduced intensity with respect to the E_4 spectral line. It is worth mentioning that E_{Pb1} and E_{Pb2} are convoluted due to the limited spectral resolution of the experimental setup adopted for these measurements (i.e., ~ 4 nm). While the presence of the relevant Pb-related lines confirms the excitability of the optical centers at >3 eV excitation energy, their decreased intensity is compatible with the predicted ionization energy of ~ 2.6 – 2.71 eV of the negative charge state of the PbV center.^{35,37} This interpretation is in agreement with the low PL intensity of the spectral features in the 550–560 nm range observed under 450 nm laser excitation at 4 K.³⁵ Such features should be identified with the E_{Pb1} and E_{Pb2} lines reported here.

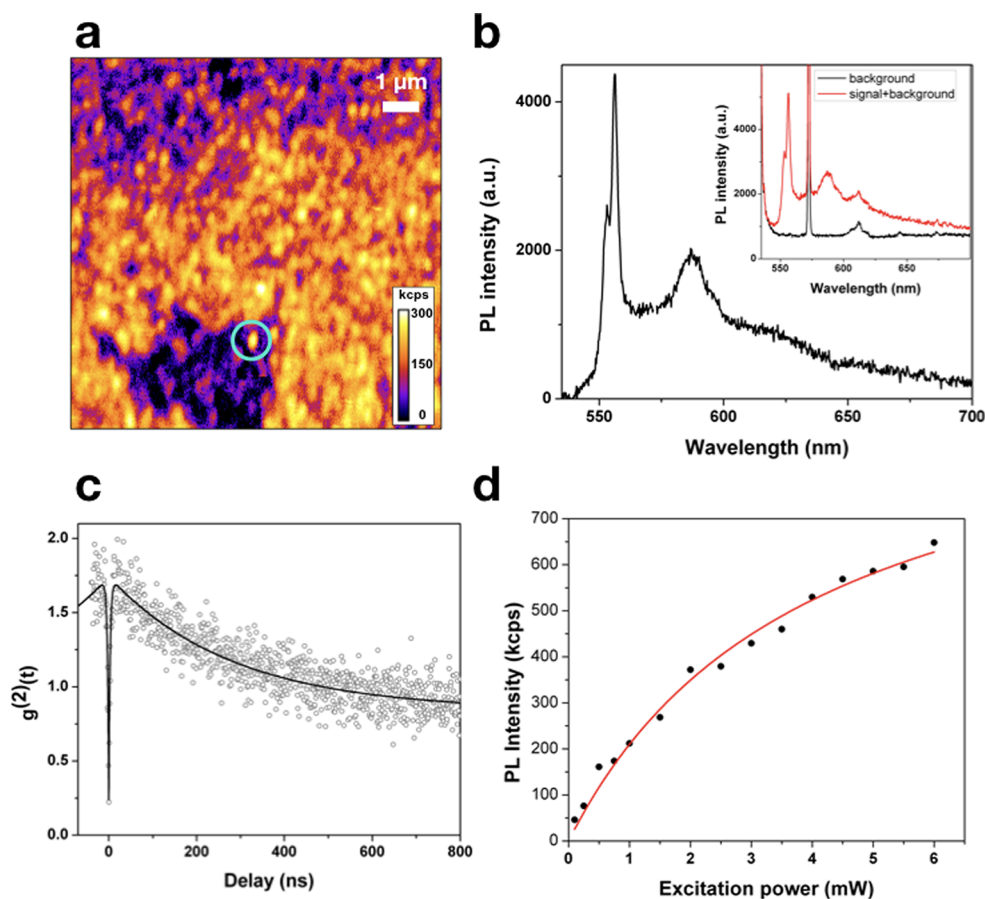


Figure 5. (a) Background-subtracted confocal PL map acquired under 532 nm laser excitation from a region implanted with PbO_2^- at $5 \times 10^{10} \text{ cm}^{-2}$ fluence. (b) Background-subtracted PL spectrum acquired from the isolated spot circled in blue in (a). The spectrum acquired from the spot and the background spectrum are displayed in the inset (black and red line, respectively). (c) Background-subtracted measurement of the second-order autocorrelation function acquired from the same spot. The black line indicates the corresponding three-level model fitting function. (d) Emission rate of an individual Pb-related defect as a function of the 532 nm laser excitation power. The red line represents the fitting curve.

Furthermore, the E_5 (641.8 nm at room temperature) and E_6 (647.8 nm) emissions are visible, together with a less intense additional feature at 670.8 nm. These lines, which are also reported from Pb-implanted diamond under 450 nm laser excitation at 4 K,³⁵ are not observable under 532 and 514 nm excitations at room temperature and barely detectable at 143 K under the same excitation wavelengths, while they instead represent the main spectral components of an articulated series of peaks in the 600–700 nm range under 405 nm excitation. While several radiation-induced defects have been studied in this spectral region,¹⁶ to the best of the authors' knowledge no simultaneous detection of both E_5 and E_6 has been reported so far. In our view, the tentative attribution of E_5 to the negative charge state of the NV center (638 nm) in ref 35 is not sufficiently convincing, since no apparent phonon sidebands could be detected and since the NV⁻ center is ionized (and therefore not optically active) under 405 nm excitation.⁴⁵ Therefore, their attribution to Pb-related defects cannot be ruled out, although such an attribution is still fairly tentative and undoubtedly requires further verification. The significant increase in the E_5 and E_6 lines' intensity under higher excitation energy might also suggest their interpretation as a different charge state of the same defect(s) associated with the $E_{\text{Pb1}}-E_{\text{Pb2}}$ emission.

■ SINGLE-PHOTON PL EMISSION

Spectral Analysis. The photoluminescence of Pb-related defects was characterized at the single-photon emitter level at the outer edge of a region implanted with PbO_2^- ions at $5 \times 10^{10} \text{ cm}^{-2}$ fluence (sample #1). PL maps were acquired using a confocal microscope under 532 nm CW laser excitation (0.5 mW power on the sample surface) and a set of optical filters, thus enabling the collection of photons at >550 nm wavelengths. A systematic investigation under 405 nm laser excitation was not possible due to the significantly attenuated PL intensity of the relevant emission lines (E_{Pb1} , E_{Pb2} , E_3), possibly due to the ionization of the defect. Figure 5a displays a typical PL map, in which individual emitting spots are distributed with a $\sim 1 \mu\text{m}^{-2}$ areal density. Assuming a reduction in the Pb concentration of a factor of ~ 10 with respect to the region implanted at the nominal fluence value, a preliminary estimation of the Pb-related centers' formation efficiency under the adopted thermal processing parameters results in a $\sim 2\%$ value, which is approximately in line with previous reports in the scientific literature on group-IV-related impurities.^{26,32} A dedicated study relying on a deterministic implantation process would provide a more accurate estimation of the efficiency and thus enable optimizing the thermal annealing process to further enhance this parameter.

Figure 5b shows the room-temperature emission spectrum acquired from the bright spot highlighted by the green circle in

Figure 5a. The background spectrum acquired from an unimplanted region was subtracted from the reported spectrum to suppress the first- (572 nm) and second-order (~610–620 nm) Raman scattering features; the unprocessed spectra are visible in the inset of **Figure 5b**. The emitter exhibited both the $E_{\text{pb}1}$ and $E_{\text{pb}2}$ lines, with a clear spectral separation at room temperature. Conversely, the attribution of the E_3 line could not be further addressed, as its emission was filtered out with the adopted >550 nm spectral filtering. On the other hand, its splitting at low temperatures might also indicate a common origin from the very same Pb defect responsible for the $E_{\text{pb}1}$ and $E_{\text{pb}2}$ emissions. The concurrent observation of the $E_{\text{pb}1}$ and $E_{\text{pb}2}$ PL peaks at the single-photon emitter level offers further elements for their attribution, although three different interpretations could be justified on the basis of the theoretical models available from the literature.^{35,37}

The spectral position of the PbV ZPL at ~517 nm predicted in ref 37 is not compatible with the data presented in this work. On the other hand, the model reported in ref 35 indicates an intermediate value (~544 nm) between the experimental lines $E_{\text{pb}1}$ and E_3 , so that it cannot be regarded as a useful disambiguation. As a first hypothesis, the $E_{\text{pb}1}$ and $E_{\text{pb}2}$ lines (spectral separation: ~17.5 meV) could be interpreted as a ZPL doublet, based on the prominence of their stronger intensity with respect to the other spectral features at room temperature. This attribution would be consistent with the theoretical prediction of a 4.4 THz (~18.7 meV) ground state splitting reported in ref 37. According to this interpretation, the E_3 doublet line might correspond to a different Pb-related complex which is dissociated at higher annealing temperatures, similarly to the 593.5 nm emission in Sn-implanted diamond.^{32,33} Alternatively, the sole $E_{\text{pb}1}$ line might be regarded as the ZPL, while the $E_{\text{pb}2}$ would be its phonon replica associated with quasi-local vibrations. This hypothesis is compatible with the expression of the energy shift associated with the interaction with quasi-local vibrations:^{16,32,46}

$$\Delta E = [m/3/(M - m)]^{1/2} \omega_D \quad (1)$$

where $\omega_D = 150$ meV is the Debye frequency of diamond and $m = 12$ and $M = 207.2$ are the atomic weights of C and Pb, respectively. In this case the energy for the quasi-local vibration is predicted to be ~21.5 meV, in satisfactory agreement with the aforementioned energy separation of ~17.5 meV observed between $E_{\text{pb}1}$ and $E_{\text{pb}2}$. On the other hand, this attribution does not support the prediction of a significant ground state splitting of the center predicted by ref 37. As a third alternative hypothesis, the E_3 line might be interpreted as the ZPL, and the $E_{\text{pb}1}$ and $E_{\text{pb}2}$ emissions would correspond to its phonon replicas. This interpretation is consistent with the prediction in ref 37 of strong phonon interaction in the 55–70 meV range. On the other hand, the E_3 splitting (~3 meV) observed at 143 K would be significantly smaller with respect to what is predicted theoretically in ref 37.

Notably, the absence of the E_4 line at the single-photon emitter level reinforces its attribution to the ZPL of the NV⁰ center. Interestingly, the PL spectrum at the single-photon emitter level displays a band centered at ~590 nm, also reported in ref 35 under the same excitation wavelength, rather than the whole B_{pb} band reported in **Figure 1b**. This observation suggests that the B_{pb} band results from the convolution of the E_4 emission at 575 nm with the aforementioned 590 nm band. Under this hypothesis, the 590 nm band could be interpreted as related to optical

phonons with ~145, ~155, or ~200 meV energy upon the attribution of the ZPL to the $E_{\text{pb}1}$ peak, the $E_{\text{pb}1}$ – $E_{\text{pb}2}$ doublet, or the E_3 emission, respectively.

Furthermore, no evidence of the E_4 – E_6 lines could be observed under the given experimental conditions. This observation reinforces the hypothesis that the latter spectral features might be associated with a different defect type or with a different charge state of the same complex.

Nonclassical Emission Properties. The single-photon emission characterization of the probed spot was performed by measuring the second-order autocorrelation function $g^{(2)}(t)$ ⁴⁷ under 532 nm excitation at 0.5 mW power. **Figure 5c** displays the experimental curve obtained upon the subtraction of the above-mentioned background fluorescence associated with the Raman scattering. The optical center displayed a bunching at zero delay time. Having estimated the signal-to-background ratio as $\rho = S/(S + B) = 0.52$, the histogram of the measured coincidences $C(t)$ was corrected according to the following expression:⁴⁷

$$g^{(2)}(t) = (C(t) - (1 - \rho^2))/\rho^2 \quad (2)$$

The corrected value $g^2(t = 0) < 0.5$ indicates evidence of nonclassical emission from the Pb-related center under consideration. The emitter also displayed a significant bunching behavior, which was interpreted in terms of a three-level system according to the fitting function³²

$$f(t) = 1 - (1 - a_1) \exp(-|t|/\tau_1) + a_2 \exp(-|t|/\tau_2) \quad (3)$$

The characteristic time associated with the antibunching behavior was estimated as $\tau_1 = 3.0 \pm 0.6$ ns, in line with the typical emission lifetimes reported for the group-IV-related color centers in diamond.^{17,29,32,33} Similarly, Pb-related centers share with the Si-, Ge-, and Sn-related centers a three-level structure.^{17,32} We cannot rule out that this observation might originate from an interplay between the $E_{\text{pb}1}$ / $E_{\text{pb}2}$ doublet with the E_3 emission line, e.g., resulting from an incomplete annealing of the defect under the adopted thermal processing of the substrate.

Figure 5d shows the typical trend of the background-subtracted PL emission intensity I as a function of the laser excitation power P , as acquired from an individual Pb-related center exhibiting a photostable emission. The background was determined by measuring the PL count rate from an unimplanted region under the same experimental conditions. The trend was fitted with the expression³²

$$I(P) = I_{\text{sat}} P(P + P_{\text{sat}})^{-1} \quad (4)$$

where the saturation PL intensity and excitation power P_{sat} were determined as $I_{\text{sat}} = (1.04 \pm 0.07) \times 10^6$ photons s⁻¹ and $P_{\text{sat}} = 4.0 \pm 0.5$ mW, respectively.

CONCLUSIONS

We reported on the formation of optically active centers upon the introduction of Pb impurities by Pb⁻ and PbO₂⁻ ion implantation into both optical- and electronic-grade CVD diamond samples. The emission intensity of the observed PL lines in the 535–675 nm spectral range strongly correlates with the implantation fluence, thus providing a solid indication that such emission originates from stable Pb-containing lattice defects.

From a spectral analysis carried out at the ensemble level, several emission features were identified, i.e., an intense

doublet at 552.1 nm (labeled as E_{Pb1}) and 556.8 nm (E_{Pb2}), less intense lines at 539.4 nm (E_3) and 574.5 nm (E_4), and a band comprised between 565 and 600 nm (B_{Pb}). While the E_4 emission was attributed to the NV^0 ZPL emission on the basis of temperature-dependent measurements, three alternative attributions of the other above-mentioned features were extensively discussed on the basis of theoretical models and preliminary results available from the literature.^{35,37} Furthermore, two intense emission peaks at 641.8 and 647.8 nm (E_5 , E_6), barely excitable under 514 nm excitation, were observed under 405 nm excitation and were tentatively attributed to alternative charge state(s) of the same defect complex that is responsible for the $E_{\text{Pb1}}-E_{\text{Pb2}}$ emission lines.

The Pb-related luminescence was also measured from individual lattice defects, through the identification of nonclassical emission in second-order autocorrelation measurements in confocal microscopy.

Temperature-dependent spectral measurements indicated a thermal shift of the order of $\sim 10 \text{ pm K}^{-1}$ for the main emission lines, which is in line with the other demonstrated nanoscale sensors related with group-IV impurities in diamond.^{40–42}

These results represent a significant step toward completing the interpretational framework on the optical activity of diamond defects related to group IV impurities. Future studies on the defects' properties at the single-photon emitter level could lead to appealing perspectives in the fields of quantum information processing and quantum sensing. Furthermore, from a fundamental point of view, the mapping and thorough understanding of a general pattern in the opto-physical properties of color centers associated with impurities of the whole group IV could provide an important reference for the study of defects related to other chemical species.

AUTHOR INFORMATION

Corresponding Author

*E-mail: forneris@to.infn.it.

ORCID

M. Signorile: 0000-0003-0521-3702

J. Forneris: 0000-0003-2583-7424

Author Contributions

[†]S. Ditalia Tchernij and T. Lühmann contributed equally to this work.

Notes

The authors declare no competing financial interest.

ACKNOWLEDGMENTS

This research activity was supported by the following projects: “DIESIS” project funded by the Italian National Institute of Nuclear Physics (INFN) - CSN5 within the “Young Research Grant” scheme; Coordinated Research Project “F11020” of the International Atomic Energy Agency (IAEA); Project “Piemonte Quantum Enabling Technologies” (PiQuET), funded by the Piemonte Region within the “Infra-P” scheme (POR-FESR 2014-2020 program of the European Union); and “Departments of Excellence” (L. 232/2016), funded by the Italian Ministry of Education, University and Research (MIUR). The work reported in this paper was partially funded by projects EMPIR 17FUN06 “SIQUST” and 17FUN01 “BeCOME; these projects received funding from the EMPIR Programme cofinanced by the Participating States and from the European Union Horizon 2020 Research and Innovation Programme. S.P. and J.M. gratefully acknowledge the support

of Volkswagen Stiftung. S.D. gratefully acknowledges the “Erasmus Traineeship 2016–2017” program for the financial support for access to the ion implantation facilities of the University of Leipzig. Support from Compagnia di San Paolo and University of Turin, through the program 2013–2015 (Open Access Raman Laboratory) is gratefully acknowledged.

REFERENCES

- (1) Prawer, S.; Aharonovich, I. *Quantum Information Processing with Diamond: Principles and Applications*; Woodhead Publishing, 2014.
- (2) Aharonovich, I.; Englund, D.; Toth, M. Solid-state single-photon emitters. *Nat. Photonics* **2016**, *10*, 631.
- (3) Pezzagna, S.; Rogalla, D.; Wildanger, D.; Meijer, J.; Zaitsev, A. Creation and nature of optical centres in diamond for single-photon emission—overview and critical remarks. *New J. Phys.* **2011**, *13*, No. 035024.
- (4) Schröder, T.; Mouradian, S. L.; Zheng, J.; Trusheim, M. E.; Walsh, M.; Chen, E. H.; Li, L.; Bayn, I.; Englund, D. Quantum nanophotonics in diamond. *J. Opt. Soc. Am. B* **2016**, *33* (4), B65.
- (5) Orwa, J. O.; Greentree, A. D.; Aharonovich, I.; Alves, A. D. C.; Van Donkelaar, J.; Stacey, A.; Prawer, S. Fabrication of single optical centres in diamond—a review. *J. Lumin.* **2010**, *130*, 1646.
- (6) Forneris, J.; Tengattini, A.; Ditalia Tchernij, S.; Picollo, F.; Battiato, A.; Traina, P.; Degiovanni, I. P.; Moreva, E.; Brida, G.; Grilj, V.; Skukan, N.; Jakšić, M.; Genovese, M.; Olivero, P. Creation and characterization of He-related color centers in diamond. *J. Lumin.* **2016**, *179*, 59.
- (7) Sandstrom, R.; Ke, L.; Martin, A.; Wang, Z.; Kianinia, M.; Green, B.; Gao, B.; Aharonovich, I. Optical properties of implanted Xe color centers in diamond. *Opt. Commun.* **2018**, *411*, 182.
- (8) John, R.; Lehnert, J.; Mensing, M.; Spemann, D.; Pezzagna, S.; Meijer, J. Bright optical centre in diamond with narrow, highly polarised and nearly phonon-free fluorescence at room temperature. *New J. Phys.* **2017**, *19*, No. 053008.
- (9) Gaebel, T.; Popa, I.; Gruber, A.; Domhan, M.; Jelezko, F.; Wrachtrup, J. Stable single-photon source in the near infrared. *New J. Phys.* **2004**, *6*, 98.
- (10) Aharonovich, I.; Castelletto, S.; Simpson, D. A.; Stacey, A.; McCallum, J.; Greentree, A. D.; Prawer, S. Two-Level Ultrabright Single Photon Emission from Diamond Nanocrystals. *Nano Lett.* **2009**, *9*, 3191.
- (11) Gatto Monticone, D.; Traina, P.; Moreva, E.; Forneris, J.; Olivero, P.; Degiovanni, I. P.; Taccetti, F.; Giuntini, L.; Brida, G.; Amato, G.; Genovese, M. Native NIR-emitting single colour centres in CVD diamond. *New J. Phys.* **2014**, *16*, No. 053005.
- (12) Doherty, M. W.; Manson, N. B.; Delaney, P.; Jelezko, F.; Wrachtrup, J.; Hollenberg, L. C. L. The nitrogen-vacancy colour centre in diamond. *Phys. Rep.* **2013**, *528*, 1.
- (13) Maze, J. R.; Stanwix, P. L.; Hodges, J. S.; Hong, S.; Taylor, J. M.; Cappellaro, P.; Jiang, L.; Dutt, M. V. G.; Togan, E.; Zibrov, A. S.; Yacoby, A.; Walsworth, R. L.; Lukin, M. D. Nanoscale magnetic sensing with an individual electronic spin in diamond. *Nature* **2008**, *455*, 644.
- (14) Müller, T.; Aharonovich, I.; Lombez, L.; Alaverdyan, Y.; Vamvakas, A. N.; Castelletto, S.; Jelezko, F.; Wrachtrup, J.; Prawer, S.; Atatüre, M. Wide-range electrical tunability of single-photon emission from chromium-based colour centres in diamond. *New J. Phys.* **2011**, *13*, No. 075001.
- (15) Storteboom, J.; Dolan, P.; Castelletto, S.; Li, X.; Gu, M. Lifetime investigation of single nitrogen vacancy centres in nano-diamonds. *Opt. Express* **2015**, *23*, 11327.
- (16) Zaitsev, A. M. *Optical Properties of Diamond*; Springer: New York, 2001.
- (17) Wang, C.; Kurtsiefer, C.; Weinfurter, H.; Burchard, B. Single photon emission from SiV centres in diamond produced by ion implantation. *J. Phys. B: At., Mol. Opt. Phys.* **2006**, *39*, 37.

- (18) Li, K.; Zhou, Y.; Rasmita, A.; Aharonovich, I.; Gao, W. B. Nonblinking Emitters with Nearly Lifetime-Limited Linewidths in CVD Nanodiamonds. *Phys. Rev. Appl.* **2016**, *6*, No. 024010.
- (19) Rogers, L. J.; Jahnke, K. D.; Teraji, T.; Marseglia, L.; Müller, C.; Naydenov, B.; Schaffert, H.; Kranz, C.; Isoya, J.; McGuinness, L. P.; Jelezko, F. Multiple intrinsically identical single-photon emitters in the solid state. *Nat. Commun.* **2014**, *5*, 4739.
- (20) Sipahigil, A.; Jahnke, K. D.; Rogers, L. J.; Teraji, T.; Isoya, J.; Zibrov, A. S.; Jelezko, F.; Lukin, M. D. Indistinguishable Photons from Separated Silicon-Vacancy Centers in Diamond. *Phys. Rev. Lett.* **2014**, *113*, 113602.
- (21) Rogers, L. J.; Jahnke, K. D.; Metsch, M. H.; Sipahigil, A.; Binder, J. M.; Teraji, T.; Sumiya, H.; Isoya, J.; Lukin, M. D.; Hemmer, P.; Jelezko, F. All-Optical Initialization, Readout, and Coherent Preparation of Single Silicon-Vacancy Spins in Diamond. *Phys. Rev. Lett.* **2014**, *113*, 263602.
- (22) Müller, T.; Hepp, C.; Pingault, B.; Neu, E.; Gsell, S.; Schreck, M.; Sternschulte, H.; Steinmüller-Nethl, D.; Becher, C.; Atatüre, M. Optical signatures of silicon-vacancy spins in diamond. *Nat. Commun.* **2014**, *5*, 3328.
- (23) Becker, J. N.; Görlitz, J.; Arend, C.; Markham, M.; Becher, C. Ultrafast all-optical coherent control of single silicon vacancy colour centres in diamond. *Nat. Commun.* **2016**, *7*, 13512.
- (24) Zhou, Y.; Rasmita, A.; Li, K.; Xiong, O.; Aharonovich, I.; Gao, W.-b. Coherent control of a strongly driven silicon vacancy optical transition in diamond. *Nat. Commun.* **2017**, *8*, 14451.
- (25) Riedrich-Möller, J.; Arend, C.; Pauly, C.; Mücklich, F.; Fischer, M.; Gsell, S.; Schreck, M.; Becher, C. Deterministic Coupling of a Single Silicon-Vacancy Color Center to a Photonic Crystal Cavity in Diamond. *Nano Lett.* **2014**, *14* (9), 5281.
- (26) Schröder, T.; Trusheim, M. E.; Walsh, M.; Li, L.; Zheng, J.; Schukraft, M.; Sipahigil, A.; Evans, R. E.; Sukachev, D. D.; Nguyen, C. T.; Pacheco, J. L.; Camacho, R. M.; Bielejec, E. S.; Lukin, M. D.; Englund, D. Scalable focused ion beam creation of nearly lifetime-limited single quantum emitters in diamond nanostructures. *Nat. Commun.* **2017**, *8*, 15376.
- (27) Marseglia, L.; Saha, K.; Ajoy, A.; Schröder, T.; Englund, D.; Jelezko, F.; Walsworth, R.; Pacheco, L.; Perry, D. L.; Bielejec, E. S.; Cappellaro, P. Bright nanowire single photon source based on SiV centers in diamond. *Opt. Express* **2018**, *26*, 81.
- (28) Lagomarsino, S.; Flatae, A. M.; Sciortino, S.; Gorelli, F.; Santoro, M.; Tantussi, F.; De Angelis, F.; Gelli, N.; Taccetti, F.; Giuntini, L.; Agio, M. Optical properties of silicon-vacancy color centers in diamond created by ion implantation and post-annealing. *Diamond Relat. Mater.* **2018**, *84*, 196.
- (29) Iwasaki, T.; Ishibashi, F.; Miyamoto, M.; Doi, Y.; Kobayashi, S.; Miyazaki, T.; Tahara, K.; Jahnke, K. D.; Rogers, L. J.; Naydenov, B.; Jelezko, F.; Yamasaki, S.; Nagamachi, S.; Inubushi, T.; Mizuocho, N.; Hatano, M. Germanium-Vacancy Single Color Centers in Diamond. *Sci. Rep.* **2016**, *5*, 12882.
- (30) Palyanov, Y. N.; Kupriyanov, I. N.; Borzdov, Y. M.; Surovtsev, N. V. Germanium: a new catalyst for diamond synthesis and a new optically active impurity in diamond. *Sci. Rep.* **2015**, *5*, 14789.
- (31) Siyushev, P.; Metsch, M. H.; Ijaz, A.; Binder, J. M.; Bhaskar, M. K.; Sukachev, D. D.; Sipahigil, A.; Evans, R. E.; Nguyen, C. T.; Lukin, M. D.; Hemmer, P. R.; Palyanov, Y. N.; Kupriyanov, I. N.; Borzdov, Y. M.; Rogers, L. J.; Jelezko, F. Optical and microwave control of germanium-vacancy center spins in diamond. *Phys. Rev. B: Condens. Matter Mater. Phys.* **2017**, *96*, No. 081201.
- (32) Ditalia Tchernij, S.; Herzog, T.; Forneris, J.; Kupper, J.; Pezzagna, S.; Traina, P.; Moreva, E.; Degiovanni, I. P.; Brida, G.; Skukan, N.; Genovese, M.; Jaksic, M.; Meijer, J.; Olivero, P. Single-Photon-Emitting Optical Centers in Diamond Fabricated upon Sn Implantation. *ACS Photonics* **2017**, *4*, 4–2580.
- (33) Iwasaki, T.; Miyamoto, Y.; Taniguchi, T.; Siyushev, P.; Metsch, M. H.; Jelezko, F.; Hatano, M. Tin-Vacancy Quantum Emitters in Diamond. *Phys. Rev. Lett.* **2017**, *119*, 253601.
- (34) Ekimov, E. A.; Lyapin, S. G.; Kondrin, M. V. Tin-vacancy color centers in micro- and polycrystalline diamonds synthesized at high pressures. *Diamond Relat. Mater.* **2018**, *87*, 223.
- (35) Trusheim, M. E.; Wan, N. H.; Chen, K. C.; Ciccarino, C. J.; Sundararaman, R.; Malladi, G.; Bersin, E.; Walsh, M.; Lienhard, B.; Bakhr, H.; Narang, P.; Englund, D. Lead-Related Quantum Emitters in Diamond. *arXiv* **2018**, 1805, 12202.
- (36) Middleton, R. A. *Negative Ion Cookbook*; University of Pennsylvania, 1989.
- (37) Thiering, G.; Gali, A. Ab Initio Magneto-Optical Spectrum of Group-IV Vacancy Color Centers in Diamond. *Phys. Rev. X* **2018**, *8*, No. 021063.
- (38) Lohrmann, A.; Pezzagna, S.; Dobrinets, I.; Spinicelli, P.; Jacques, V.; Roch, J.-F.; Meijer, J.; Zaitsev, A. M. Diamond based light-emitting diode for visible single-photon emission at room temperature. *Appl. Phys. Lett.* **2011**, *99*, 251106.
- (39) Doherty, M. W.; Acosta, V. M.; Jarmola, A.; Barson, M. S. J.; Manson, N. B.; Budker, D.; Hollenberg, L. C. L. Temperature shifts of the resonances of the NV⁻ center in diamond. *Phys. Rev. B: Condens. Matter Mater. Phys.* **2014**, *90*, No. 041201.
- (40) Nguyen, C. T.; Evans, R. E.; Sipahigil, A.; Bhaskar, M. K.; Sukachev, D. D.; Agafonov, V. N.; Davydov, V. A.; Kulikova, L. F.; Jelezko, F.; Lukin, M. D. All-optical nanoscale thermometry with silicon-vacancy centers in diamond. *Appl. Phys. Lett.* **2018**, *112*, 203102.
- (41) Fan, J.-W.; Cojocaru, I.; Becker, J.; Fedotov, I. V.; Alkahtani, M. H. A.; Alajlan, A.; Blakley, S.; Rezaee, M.; Lyamkina, A.; Palyanov, Y. N.; Borzdov, Y. M.; Yang, Y.-P.; Zheltikov, A.; Hemmer, P.; Akimov, A. V. Germanium-Vacancy Color Center in Diamond as a Temperature Sensor. *ACS Photonics* **2018**, *5*, 765.
- (42) Alkahtani, M.; Cojocaru, I.; Liu, X.; Herzog, T.; Meijer, J.; Kupper, J.; Lühmann, T.; Akimov, A. V.; Hemmer, P. R. Tin-vacancy in diamonds for luminescent thermometry. *Appl. Phys. Lett.* **2018**, *112*, 241092.
- (43) Chen, X.-D.; Dong, C.-H.; Sun, F.-W.; Zou, C.-L.; Cui, J.-M.; Han, Z.-F.; Guo, G.-C. Temperature dependent energy level shifts of nitrogen-vacancy centers in diamond. *Appl. Phys. Lett.* **2011**, *99*, 161903.
- (44) Zaitsev, A. M. High energy ion implantation into diamond and cubic boron nitride. *Nucl. Instrum. Methods Phys. Res., Sect. B* **1991**, *62*, 81.
- (45) Aslam, N.; Waldherr, G.; Neumann, P.; Jelezko, F.; Wrachtrup, J. Photo-induced ionization dynamics of the nitrogen vacancy defect in diamond investigated by single-shot charge state detection. *New J. Phys.* **2013**, *15*, No. 013064.
- (46) Brout, R.; Visscher, W. Suggested Experiment on Approximate Localized Modes in Crystals. *Phys. Rev. Lett.* **1962**, *9*, 54.
- (47) Brouri, R.; Beveratos, A.; Poizat, J. P.; Grangier, P. Photon antibunching in the fluorescence of individual color centers in diamond. *Opt. Lett.* **2000**, *25*, 1294.